

## Carbon and Nitrogen Basicity of Aminothiophenes and Anilines

Alessandro Bagno<sup>\*,†</sup> and François Terrier<sup>‡</sup>

Centro CNR Meccanismi Reazioni Organiche, Dipartimento di Chimica Organica, Università di Padova, via Marzolo 1, 35131 Padova, Italy, and Laboratoire SIRCOB, ESA CNRS, 8086 Institut Lavoisier-Franklin, 45 Avenue des Etats-Unis, 78035 Versailles Cedex, France

Received: February 5, 2001; In Final Form: April 27, 2001

The protonation site, aromaticity, charge distribution, and NMR properties of 3-aminothiophene, 3,4-diaminothiophene, aniline, and 1,2-benzenediamine have been investigated by means of quantum chemical calculations both for the isolated and solvated species (in water and DMSO). For the isolated species (G3(MP2) level), the C-protonated form of aminothiophenes is more stable than the N-protonated form (by 5–9 kcal/mol), whereas the stability order of the protonated forms of anilines is reversed, with a closer energy balance (2–5 kcal/mol). In water or DMSO the stability of the C- and N-protonated forms of aminothiophenes is essentially the same (as obtained by a combination of G3(MP2) and DFT-IPCM solution data), whereas for anilines a strong preference for N-protonation is borne out. However, a comparison of experimental and calculated <sup>13</sup>C NMR chemical shifts shows N-protonation to be the major process in solution. While the aromaticity of the two ring types (as probed by nucleus-independent chemical shifts) is very similar, the larger nucleophilicity of the C-2 atom of aminothiophenes as compared to anilines is shown to arise from a strong polarization of the C-2–C-3 bond.

### Introduction

Amino-substituted arenes (e.g., aniline) possess two major basic/nucleophilic sites, i.e., the nitrogen atom and one of the carbon atoms in the aromatic ring. In fact, although anilines are established nitrogen bases in solution, their nucleophilic reactivity is dominated by attack onto a ring carbon, as in the Friedel–Crafts and related reactions. Moreover, in the gas phase, even the acid–base behavior has not been unambiguously established, and the protonation site of aniline has been the subject of several experimental and theoretical papers.<sup>1–7</sup> Earlier data, obtained from an analysis of substituent effects on anilines and relatively low-level calculations, were in favor of N-protonation, albeit with a small energy gap of 1–3 kcal/mol.<sup>1</sup> Subsequent experimental studies (again based on trends in substituent effects)<sup>2</sup> indicated ring protonation for some substituted anilines, and N-protonation for aniline itself. More sophisticated mass-spectroscopic studies<sup>3</sup> as well as recent theoretical results<sup>4,5</sup> were again in favor of N-protonation. Recently, however, Russo et al.<sup>6</sup> carried out an extensive computational investigation of the problem, and showed that the energy gap between the C- and N-protonated forms is very sensitive to the theoretical method employed. Thus, density-functional and MP4 methods indicate preferential C-protonation (at C-4, the para carbon atom), whereas MP2 and G2(MP2) methods yield the opposite result (N-protonation). However, even at the highest levels reported (MP4 and G2(MP2)) the energy gap is only 0.5–0.7 kcal/mol. Lately, Beauchamp et al.<sup>7</sup> also reinvestigated the problem running FT-ICR spectra of hydrated anilinium ions in nanodroplets and found that mass-spectral patterns of water clusters surrounding variously substituted anilinium ions exhibit features that can be related to

the protonation site. Thus, it was concluded that the unsubstituted, *p*-ethyl- and *N*-methyl-anilinium ions are N-protonated, whereas the *m*-thiomethylanilinium ion is ring protonated in this microsolvated environment.

Bagno et al. investigated the acid–base behavior of aniline and a series of simple amines.<sup>8</sup> Thus, they reported on the changes in the calculated electric field gradient and nuclear shielding at the nitrogen nucleus in the neutral and protonated species, and compared these with the experimentally determined changes in <sup>14</sup>N chemical shifts and NMR relaxation rates in aqueous solution. They then confirmed, among other things, that the available NMR data were consistent with the established N-protonation of aniline in solution.

Thus, the basic and nucleophilic properties of aniline are centered on different atoms (i.e., nitrogen and a ring carbon, respectively). However, functionally similar species such as aminothiophenes, despite a superficial resemblance, reportedly behave differently from anilines in many respects. In particular, much evidence has been accumulated that 3-aminothiophenes are remarkably more prone to undergo electrophilic substitution at a ring carbon position than at the amino nitrogen.<sup>9–12</sup> The basicity and nucleophilicity of 3-aminothiophene, 3,4-diaminothiophene and their *N*-methylated derivatives were recently investigated by Terrier et al., in comparison with the behavior of the corresponding anilines.<sup>13,14</sup> Data obtained through <sup>1</sup>H NMR and potentiometric studies have provided clear evidence that these compounds behave as nitrogen bases in H<sub>2</sub>O–DMSO mixtures, as well as in pure DMSO. The p*K* values for this acid–base process have been measured and found to compare well with those for structurally related anilines. Also, the nucleophilic properties were probed through the reactivity of aminothiophenes toward the strongly electrophilic reagent 4,6-dinitrobenzofuroxan (DNBF). Thus, it was found that the addition of DNBF occurs only at C-2 of the thiophene ring. The S<sub>E</sub>Ar-type reaction proceeds through rate-determining

\* To whom correspondence should be addressed. Fax: +39 0498275239. E-mail: alex@chor.unipd.it.

<sup>†</sup> Centro CNR Meccanismi Reazioni Organiche.

<sup>‡</sup> Laboratoire SIRCOB.

**TABLE 1: Gaussian-3(MP2) Energies and Proton Affinities of Aminothiophenes, Anilines, and Their Protonated Forms<sup>a</sup>**

species	<i>E</i>	$\Delta E$	H	$\Delta H$	PA
3-aminothiophene ( <b>1</b> )	-607.575 952		-607.575 008		216
<b>1C</b>	-607.920 060	(0.0)	-607.919 115	(0.0)	
<b>1N</b>	-607.906 241	8.7	-607.905 297	8.4	
3,4-diaminothiophene ( <b>2</b> )	-662.855 373		-662.854 429		219
<b>2C</b>	-663.204 074	(0.0)	-663.203 13	(0.0)	
<b>2N</b>	-663.196 307	4.9	-663.195 363	5.1	
Aniline ( <b>3</b> )	-287.107 825		-287.106 881		210 <sup>b</sup>
<b>3C</b>	-287.438 764	(0.0)	-287.437 819	(0.0)	
<b>3N</b>	-287.441 902	-2.0	-287.440 958	-1.2	
1,2-benzenediamine ( <b>4</b> )	-342.391 029		-342.390 084		215 <sup>c</sup>
<b>4C</b>	-342.724 904	(0.0)	-342.723 959	(0.0)	
<b>4N</b>	-342.733 367	-5.3	-342.732 423	-4.7	

<sup>a</sup> All data are referred to the C-protonated form. Absolute energies (*E*) and enthalpies (*H*; 298 K, 1 atm) in atomic units (au); relative energies ( $\Delta E$ ) and enthalpies ( $\Delta H$ ) in atomic units (au) and kilocalories per mole (kcal/mol), respectively. Values of  $\Delta E$  and  $\Delta H$  refer to the two protonation sites; proton affinities (PA, kcal/mol) are given for the most favorable protonation site (C for **1–2**, N for **3–4**). <sup>b</sup> Experimental PA: 210.9.<sup>29</sup> <sup>c</sup> Experimental PA: 214.3.<sup>29</sup>

formation of a zwitterionic carbon-bonded  $\sigma$  adduct and subsequent fast deprotonation, no competitive addition (or substitution) being observed at nitrogen. This behavior was ascribed to a conjunction of favorable kinetics and thermodynamic factors.

This pattern should be compared with that shown by anilines which, on the contrary, reversibly add to DNBF via the nitrogen atom before yielding the C-adduct in a subsequent slower step.<sup>15</sup> Thus, although the basic properties are common to both anilines and aminothiophenes, the carbon nucleophilicity of the latter seems to be quite enhanced. This property was empirically ascribed to a strong enaminic character of the C-2 carbon, which may be interpreted as arising from a lower aromaticity of the aminothiophene ring.<sup>14</sup>

In this paper, we report on our computational studies aimed at clarifying the preceding issues, i.e., (a) modeling the carbon and nitrogen basicity in the gas phase and in solution; (b) predicting the NMR spectral changes that can be expected upon formation of each protonated form, to provide an independent framework for interpreting experimental data; (c) understanding the factors underlying the different nucleophilic behavior of the title compounds.

## Results

The structures and energetics of protonation of 3-aminothiophene (**1**), 3,4-diaminothiophene (**2**), aniline (**3**), and 1,2-benzenediamine (**4**) at nitrogen or carbon have been investigated theoretically by means of ab initio and DFT calculations, both for the isolated species and in the solvents water and DMSO, modeled as a continuum by the IPCM method.<sup>16</sup> All calculations were carried out with *Gaussian 98*.<sup>17</sup>

**Gas-Phase Basicities.** The structures and energies of **1–4** and their C- and N-protonated forms (denoted with a C or N suffix, respectively) were first obtained at the AM1 level, thus screening the various ring protonation sites available. **1** is predicted to be a carbon (C-2) rather than a nitrogen base, although  $\Delta\Delta H_f$  is quite small (0.7 kcal/mol). We also note the much lower basicity of the sulfur atom, of C-3 (the *ipso* carbon) and C-5 (the *meta*-like position), with  $\Delta\Delta H_f = 15–30$  kcal/mol, which renders these atoms essentially unavailable for protonation. In contrast, **2** should preferentially undergo nitrogen protonation, although the  $\Delta\Delta H_f$  value is again rather small (2.5 kcal/mol). On the contrary, for both **3** and **4** the nitrogen is the most basic site, and the energy gap with respect to C-4 is slightly higher (2–6 kcal/mol). Again, the *ipso* and *meta* carbons (C-1 and C-3) are much less basic (by 30–40 kcal/mol) and can be safely ruled out. Since protonation at C-2 (**1** and **2**) or C-4 (**3**

and **4**) leads to the most stable C-protonated form, all further calculations were run on these species only.

High-level structures and energies for the above species were then obtained with Gaussian-3 theory using reduced Møller–Plesset order<sup>18,19</sup> (G3(MP2) in shorthand), which has been recently proposed as a more efficient alternative to G2(MP2) theory, while maintaining a small deviation in the calculated proton affinities of the test set. This level effectively amounts to a calculation of the energy at the QCISD(T)(full) level by making various additivity assumptions, and includes a geometry optimization at the MP2(full)/6-31G(d) level; such geometries were subsequently employed in further calculations. G3(MP2) energies are reported in Table 1, while the structures are graphically sketched in Chart 1. Optimized structures are given in the Supporting Information as PDB files.

**Basicities in Solution and Solvation Energetics.** The solvation of the protonated species was investigated by the Isodensity Polarizable Continuum Method (IPCM), which treats the solvent as a continuum of given dielectric permittivity  $\epsilon$ .<sup>16</sup> This method was found to be quite effective in predicting the relative energies of a wide array of tautomeric ions formed by protonation of the alternative sites in polyfunctional bases and acids.<sup>8,20–23</sup>

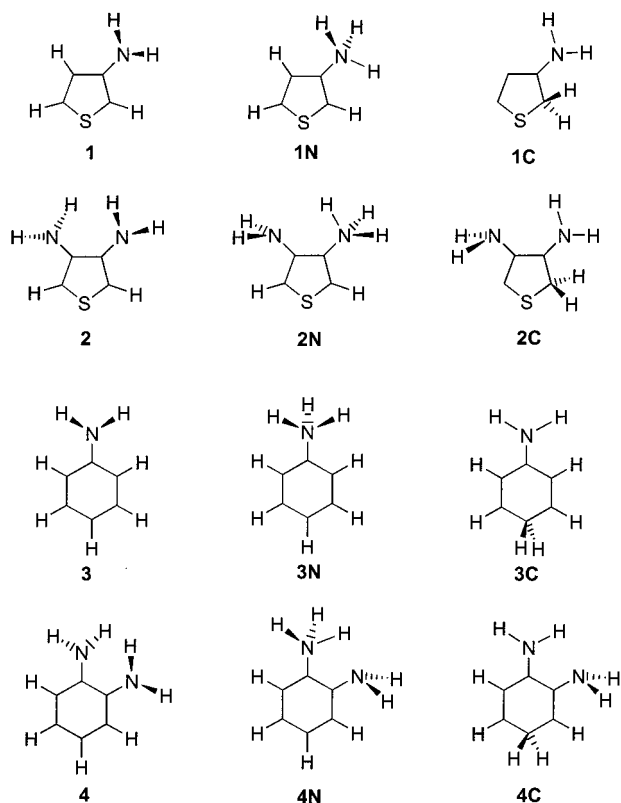
Since gradients are not available for this method, the previous G3(MP2) geometries were employed; calculations were run both for water ( $\epsilon = 78.3$ ) and DMSO ( $\epsilon = 46.7$ ) as solvents. These results are collected in Table 2 (only for water, since the corresponding data for DMSO differ only by ca. 0.1 kcal/mol). However, owing to the inherently iterative nature of the calculations, use of an MP2 wave function (as in the gas-phase calculations) was deemed too expensive, and we resorted to using a DFT method (Becke's hybrid three-parameter functional with Lee–Yang–Parr correlation, B3LYP<sup>24</sup>) with the larger 6-311++G(2d,2p) basis set, incorporating diffuse functions on all atoms to better model long-range interactions and two sets of polarization functions for better performance in the NMR calculations (see below). Furthermore, since the IPCM method requires a preliminary gas-phase energy calculation, we have the opportunity to further compare the performance of DFT and QCI methods, which were found to yield rather different results for anilines. However, with this approach solvation energies are calculated at a different theoretical level than gas-phase energies; hence, to consistently evaluate the transfer energy balance, we have to connect the various terms through a Born–Haber cycle.<sup>8</sup> Thus, defining the relative energies of the N- and C-protonated forms in the gas and solution phases as  $\Delta E_{(g)} = E_{(g)}^N - E_{(g)}^C$  and  $\Delta E_{(s)} = E_{(s)}^N - E_{(s)}^C$ , respectively, the thermodynamic cycle

TABLE 2: Energies in Water from the IPCM Continuum Method<sup>a</sup>

species	gas phase		water		$\Delta E_{(\text{aq})}$
	$E$	$\Delta E$	$E$	$\Delta E$	
3-aminothiophene (1)					
<b>1C</b>	-608.821 050	(0.0)	-608.915 001	(0.0)	(0.0)
<b>1N</b>	-608.803 415	11.1	-608.909 486	3.5	1.1
3,4-diaminothiophene (2)					
<b>2C</b>	-664.203 954	(0.0)	-664.294 099	(0.0)	(0.0)
<b>2N</b>	-664.188 871	9.5	-664.287 885	3.9	-0.7
aniline (3)					
<b>3C</b>	-288.047 212	(0.0)	-288.133 868	(0.0)	(0.0)
<b>3N</b>	-288.046 288	0.6	-288.149 901	-10.1	-12.6
1,2-benzenediamine (4)					
<b>4C</b>	-343.427 400	(0.0)	-343.512 898	(0.0)	(0.0)
<b>4N</b>	-343.433 600	-3.9	-343.529 499	-10.4	-11.8

<sup>a</sup> B3LYP/6-311++G(2d,2p) at the MP2(full)/6-31G(d) geometry from the G3(MP2) calculation. Absolute and relative energies in au and kcal/mol, respectively.  $\epsilon(\text{water}) = 78.3$ . The corresponding entries for DMSO ( $\epsilon = 46.7$ ) differ by  $<0.2$  kcal/mol. Values of  $\Delta E_{(\text{aq})}$  and  $\Delta E_{(\text{DMSO})}$  calculated with eq 2 (see text).

CHART 1: Structures of 3-Aminothiophene, 3,4-Diaminothiophene, Aniline, 1,2-Benzenediamine, and Their N- and C-Protonated Forms at the G3(MP2) Level (MP2(full)/6-31G(d) Geometry)



shows that the latter can be expressed as in eq 1:

$$\Delta E_{(s)} = \Delta E_{(g)} + (E_N^s - E_C^s) \quad (1)$$

where  $E_i^s$  is the solvation energy of species  $i$ , given by  $E_i^s = E_i^{\text{IPCM}} - E_i^{\text{DFT}}$ , in turn given by the energy difference in solution (from an IPCM calculation) and in the gas phase (from the corresponding DFT calculation, obtained in the same job). On the other hand, our best estimate of the gas-phase energy is by G3(MP2) calculations, as seen before. Hence, the required term is given by eq 2, where  $s = \text{water}$  or  $\text{DMSO}$ .

$$\Delta E_{(s)} = (E_N - E_C)^{\text{G3MP2}} + (E_N - E_C)^{\text{IPCM}} - (E_N - E_C)^{\text{DFT}} \quad (2)$$

**NMR Properties.** The pattern of change of the main NMR properties (i.e., the chemical shift and, for quadrupolar nuclei like  $^{14}\text{N}$ , the relaxation rate) was previously demonstrated to be a versatile and powerful means to pinpoint the most stable ionized form of polyfunctional bases and acids.<sup>8,20–23,25</sup> Thus, for instance, the large decrease in the longitudinal relaxation rate of the  $^{14}\text{N}$  nucleus in ammonium ions, compared to that of neutral amines, was found to be a useful probe of the state of ionization of amines.<sup>8,25</sup> However, owing to the often capricious nature of such spectral changes, it was found that a theoretical prediction of the change in the sought parameters is necessary. Such predictions are nowadays easily performed by means of quantum-chemistry methods, which allow to calculate the molecular properties lying at the root of the NMR spectral features, i.e., the nuclear shielding and the electric field gradient (which are connected to the chemical shift and the longitudinal relaxation rate, respectively).

To this effect, we ran such calculations for **1–4** and their protonated forms, the results of which are given as follows.  $^{13}\text{C}$  and  $^{14}\text{N}$  chemical shifts are reported both as absolute shielding constants ( $\sigma$ ) and as chemical shift changes  $\Delta\delta = \sigma(\text{B}) - \sigma(\text{BH}^+)$ , which can be directly compared to experimental values (making allowance for possible solvent effects). The longitudinal relaxation rate ( $1/T_1$ ) of  $^{14}\text{N}$  in solution is determined by a combination of factors, which includes the largest component of the electric field gradient tensor  $q_{zz}$  and its asymmetry parameter  $\eta = |q_{xx} - q_{yy}|/q_{zz}$  as in  $1/T_1 \propto \chi_{\text{eff}} = \chi^2(1 + \eta^2/3)$ , where  $\chi = eQq_{zz}/h$ .<sup>25</sup> Values of  $\chi_{\text{eff}}$  for the neutral and protonated species can then be compared; all NMR results are collected in Table 3.

**Aromaticity and Charge Delocalization.** We strived to address the aromaticity issue by calculating nucleus-independent chemical shifts (NICS).<sup>26</sup> These are reported as the negative of the calculated shielding, a large negative value indicating a diamagnetic ring current and hence stronger aromaticity. Since a noticeable basis-set dependence was observed,<sup>26</sup> for consistency we repeated the calculation for the parent species (thiophene and benzene) at the same level employed so far. The amino substituents affect NICS values only to a small extent; thus, the values for **1**, **2** or **3**, **4** are more negative than those of thiophene ( $-12.7$ ) and benzene ( $-7.6$ ) by 1 ppm at most.

To define the type and extent of charge distribution within the aromatic ring, we also calculated atomic charges in the neutrals by means of a natural population analysis, based on the Natural Orbital method (NBO),<sup>27</sup> which are collected in Table 4.

**TABLE 3: Carbon and Nitrogen Shieldings and Chemical Shift Changes of Aminothiophenes, Anilines, and Their Protonated Forms<sup>a</sup>**

species	$\sigma$	$\Delta\delta$	$\chi_{\text{eff}}$	species	$\sigma$	$\Delta\delta$	$\chi_{\text{eff}}$
thiophene				benzene			
C-2	49.47	—		C	48.98	—	
C-3	51.96	—		aniline (3)			
3-aminothiophene (1)				N	183.53	—	22.38
N	193.52	—	23.00	C-1	28.51	—	
C-2	75.85	—		C-2	63.84	—	
C-3	30.02	—		C-3	48.10	—	
C-4	58.61	—		C-4	59.80	—	
C-5	48.41	—		3C			
1C				N	118.90	64.6	8.13
N	120.58	72.9	7.66	C-1	11.08	17.4	
C-2	131.91	-56.1		C-2	55.37	8.5	
C-3	-11.50	41.5		C-3	7.55	40.6	
C-4	62.04	-3.4		C-4	141.97	-82.2	
C-5	-20.77	69.2		3N			
1N				N	192.46	-8.9	0.017
N	200.36	-6.8	0.047	C-1	54.31	-25.8	
C-2	51.95	23.9		C-2	57.62	6.2	
C-3	60.58	-30.6		C-3	41.94	6.2	
C-4	60.79	-2.2		C-4	39.46	20.3	
C-5	35.29	13.1		1,2-benzenediamine (4)			
3,4-diaminothiophene (2)				N	190.34	—	20.33
N	198.29	—	21.49	C-1,2	39.97	—	
C-2,5	74.65	—		C-4,5	57.46	—	
C-3,4	39.07	—		C-3,6	62.83	—	
2C				4C			
N(3), N(4)	118.63, 228.35	avg 24.8	avg 17.5	N(1), N(2)	116.42, 208.99	avg 27.6	avg 15.5
C-2	137.93	-63.3		C-1	9.96	30.0	
C-3	-7.88	47.0		C-2	40.49	-0.5	
C-4	45.69	-6.6		C-3	25.71	37.1	
C-5	-8.47	83.1		C-4	142.19	-84.7	
2N				C-5	9.30	48.2	
N(3)	205.20	avg -15.4	avg 11.3	C-6	56.18	6.6	
N(4)	222.28			4N			
C-2	54.22	20.4		N(1), N(2)	202.37, 215.01	avg 18.3	avg 11.6
C-3	59.20	-20.1		C-1	52.87	12.9	
C-4	45.35	-6.3		C-2	41.79	1.8	
C-5	46.08	28.6		C-3	45.28	-17.5	
				C-4	39.99	-17.5	
				C-5	43.67	-13.8	
				C-6	56.26	-6.6	

<sup>a</sup> B3LYP/6-311++G(2d,2p) at the MP2(full)/6-31G(d) geometry from the G3(MP2) calculation.  $\Delta\delta = \sigma(\text{B}) - \sigma(\text{BH}^+)$ , in ppm.  $\chi_{\text{eff}} = \chi^2(1 + \epsilon^2/3)$ , in MHz<sup>2</sup> (= 10<sup>12</sup> Hz).

**TABLE 4: NBO Atomic Charges of Aminothiophenes and Anilines<sup>a</sup>**

species	$q$	species	$q$
thiophene		aniline (3)	
S	0.45	N	-0.80
C-2	-0.41	S	0.43
C-3	-0.25	C-1	0.16
3-aminothiophene (1)		C-2	-0.25
N	-0.80	C-3	-0.18
S	0.44	C-4	-0.24
C-2	-0.48	1,2-benzenediamine (4)	
C-3	0.11	N	-0.82
C-4	-0.28	C-1,2	0.13
C-5	-0.39	C-4,5	-0.22
3,4-diaminothiophene (2)		C-3,6	-0.24
N	-0.81		
C-2,5	-0.46		
C-3,4	0.095		

<sup>a</sup> B3LYP/6-311++G(2d,2p)//MP2(full)/6-31G(d).

## Discussion

**Geometrical Features.** All geometries discussed (Chart 1) have been obtained at the MP2(full)/6-31G(d) geometry including a HF/6-31G(d) vibrational analysis (part of the G3(MP2) calculation), and all structures were checked to be minima on the potential energy surface.

All neutrals feature nonplanar amino groups. In the case of **2** and **4**, where the NH hydrogens are relatively close, the twisting is opposite so as to maximize their distance. Another structure was located for **4**, which had the NH hydrogens of one group oriented toward the other amino nitrogen in an apparent hydrogen-bonding fashion; however, vibrational analysis showed it not to be a stationary point, and was discarded.

On the contrary, in C-protonated **1** and **3** (**1C** and **3C**) the amino group is planar and coplanar with the ring; for **2C** and **4C** this is observed only for the amino group ortho or para to the protonated carbon atom, whereas the other (in a meta relationship with the protonated carbon) remains nonplanar and is twisted with respect to the ring. The two amino groups remain arranged so as to suggest a hydrogen bond between them, the planar one acting as the donor, thereby contributing to the stability of these arenonium or hetarenium species.

In the N-protonated diamino species **2N** and **4N**, the unprotonated amino group is also pyramidal and twisted with respect to the ring, and arranged so as to suggest, again, a hydrogen bond to the protonated one.

**Aminothiophenes.** At the G3(MP2) level (Table 1), the energy (or the enthalpy) of ring-protonated forms (**1C**, **2C**) is lower than that of the corresponding N-protonated ones, and

the most basic site of both **1** and **2** is the C-2 carbon rather than the nitrogen, with a sizable energy gap ( $\Delta E$  or  $\Delta H = 4-8$  kcal/mol). The picture is similar if gas-phase DFT energies are considered (Table 2), except that the energy gap is larger (9–11 kcal/mol).

Taking into account the solvent effect on the protonation equilibrium (Table 2), we first note that the results obtained for DMSO or water as solvents are negligibly different, and can be discussed interchangeably (which holds also for the anilines). This is a known effect for solvents with high  $\epsilon$ .<sup>28</sup> In the solution phase, the energy gap becomes very small ( $\Delta E_{\text{aq}}$  ca. 1 kcal/mol), the results suggesting carbon and nitrogen protonation for **1** and **2**, respectively. Hence, a large solvent effect is borne out, since it levels off a substantial gas-phase energy gap of 10 kcal/mol and further asserts the strong hydration of ammonium ions compared to carbenium ions. In any event, the calculated energies in solution are too close to allow for a reliable prediction of the protonation site.

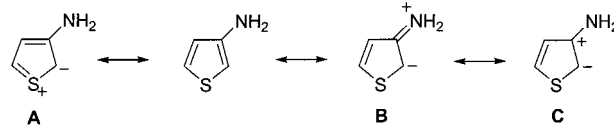
**Anilines.** At the G3(MP2) level, the energy gap between N- and C-protonated species is smaller than for thiophenes ( $\Delta E$  or  $\Delta H = 1-5$  kcal/mol), but most importantly the sign is reversed, **3N** and **4N** being now more stable. This is in qualitative agreement with the data by Russo et al.<sup>6</sup> DFT results for anilines, which indicate N-protonation of **3** to be slightly disfavored, unlike the case of **4**, for which N-protonation is borne out (although by only 4 kcal/mol). We also note the very good agreement (<1 kcal/mol) between G3(MP2) and experimental<sup>29</sup> proton affinities (Table 1).

Like in the previous case, inclusion of the solvent effect stabilizes the N-protonated form but, since the gas-phase energy balance is essentially even, the result is that both **3N** and **4N** are predicted to be substantially more stable than their C-protonated counterparts, with  $\Delta E_{\text{aq}}$  of ca. 12 kcal/mol. Thus, N-protonation is borne out, as is well-known for the aqueous solution and has been shown to hold also for water nanodroplets.<sup>7</sup>

**Changes in NMR Parameters.** The accuracy of calculated chemical shift changes upon protonation can be assessed through the comparison with experimental results for aniline, whose protonation site in solution is unambiguously established as the nitrogen atom. Thus, except for C-2 (for which calculated chemical shift changes for both **3C** and **3N** are similar), the calculated shift changes agree with the experimental results<sup>30</sup> ( $\Delta\delta = -18, +2$  and  $+14$  ppm for C-1, C-3, and C-4, respectively) only in the case of N-protonation ( $\Delta\delta(\mathbf{3N}) = -26, +6, +20$  ppm; cf.,  $\Delta\delta(\mathbf{3C}) = +17, +41, -82$  ppm; see Table 3). Hence, the theoretical level adopted is adequate to model most <sup>13</sup>C spectral changes occurring upon proton transfer.

With regard to aminothiophenes, Terrier and others reported the <sup>13</sup>C chemical shifts of the ring carbons of **1** and 3-dimethylaminothiophene, both as neutral species in DMSO and after addition of one equivalent of CH<sub>3</sub>SO<sub>3</sub>H.<sup>14,31,32</sup> Such chemical shift changes can be compared with our calculated values as follows. Calculations predicts major shielding variations for all carbon nuclei, except perhaps C-4. C-Protonation (at C-2, **1C**) is expected to cause a large shielding at C-2 ( $\Delta\delta(\text{C-2}) = -56$  ppm), whereas N-protonation (**1N**) should entail a smaller deshielding ( $\Delta\delta(\text{C-2}) = +24$  ppm). Conversely, the shift changes at C-3 are reversed in sign (deshielding for C-protonation and shielding for N-protonation, respectively). The changes at C-5 have the same sign, but the magnitude is much larger for C-protonation. Experimental results, i.e., deshielding at C-2 (ca. +21 ppm), shielding at C-3 (ca. -19 ppm), small

## CHART 2: Canonic Resonance Structures of 3-Aminothiophene (1)



deshielding at C-5 (ca. +4 ppm), are compatible only with N-protonation.

The electric field gradient (efg) at nitrogen is known to be a probe of the ionization state of the nitrogen atom, since quaternization entails a symmetry increase and hence a decrease in the efg. The latter change is reflected in an increase in the <sup>14</sup>N longitudinal relaxation time (or a decrease in the line width). For the monoamino species **1** and **3**, theoretical predictions again conform to these criteria; thus, although protonation at either site causes an efg decrease, N-protonation is connected with a much larger decrease (500–1000-fold) than C-protonation (only 3-fold). On the contrary, for the diamino species **2** and **4** theory predicts essentially the same efg change, i.e., a small decrease of about the same magnitude (ca. 2-fold) upon protonation at either site. Hence, in this case <sup>14</sup>N relaxation will not distinguish between the two processes.

**Aromaticity and Charge Distribution.** As previously mentioned, the origin of the differing nucleophilic behavior of aminothiophenes and anilines might be traced to a different degree of aromaticity or charge distribution in the ring. However, the similarity among all compounds considered indicates that, within the scope of the NICS method, a different aromaticity of the two ring types does not account for the observed differences.

The electron distribution in aminothiophenes and anilines can be analyzed in resonance terms as follows. An analysis of NBO charges (Table 4) shows that C-2 and C-5 of aminothiophenes are strongly negative ( $q \approx -0.45$ ), whereas the corresponding ortho and para carbons in anilines are much less negative ( $q \approx -0.25$ ). On the other hand, the nitrogen atoms are uniformly negative ( $q \approx -0.8$ ). Hence, the C-2 carbon in aminothiophenes is much more negatively charged than the C-2,4 ones in anilines, which accounts for its enhanced nucleophilic reactivity.

The S–C-1, C-1–C-2, and C-2–C-3 bonds in 3-aminothiophene are longer than in thiophene ( $\Delta r = 0.003-0.005$  Å), whereas the C-3–C-4 bond is shorter ( $\Delta r = -0.003$  Å) and the C-4–S bond is unchanged. Further information is also provided by <sup>13</sup>C chemical shifts, which are known to be sensitive to the electron density,<sup>9-14</sup> and thus provide complementary information to atomic charges. Calculated and experimental shift differences between thiophene and 3-aminothiophene are in very good agreement and point out a large shielding of C-2 ( $\Delta\delta = -32.4$  ppm) as well as a deshielding of C-3 ( $\Delta\delta = +21.0$  ppm), while C-4 and C-5 undergo much smaller changes. The corresponding differences between benzene and aniline are much less marked ( $\Delta\delta = 20.5, -14.8, 0.9, -10.8$  ppm for C-1, C-2, C-3, and C-4, respectively), showing that the electron density in aniline is built up to a similar extent (and hence more uniformly) at both C-2 and C-4.

When the information from atomic charges, geometry changes and chemical shifts are considered together, a decrease in the S–C-1, C-1–C-2, and C-2–C-3 bond orders, and a substantial polarization of the C-2<sup>δ-</sup>–C-3<sup>δ+</sup> bond in 3-aminothiophene are borne out. Thus, the electronic structure of **1** and **2** would be represented by the enaminic resonance hybrid **B**, **C** rather than as the sulfur-ylide one **A** (Chart 2). On the other hand, the electronic structure of aniline is substantially less polarized, since

the electron density is shared between C-2 and C-4 to the same extent. The net result is that, in the case of nucleophilic additions leading to weakly solvated products (like in the case of DNBF), aminothiophenes will react at C-2 owing to its large electron density, whereas for aniline the preference for C-2 or N will be much less marked. Conversely, protonation is strongly affected by the solvation of the ion thus formed, and in this case, the stronger solvation of the ammonium ion is the controlling factor. However, in the case of aniline both the intrinsic stability and the solvation of the anilinium ion act in the same direction, whereas in the case of aminothiophenes the intrinsic stability of the C-protonated form is larger, so that the observed behavior stems from the balance between two opposing factors.

### Concluding Remarks

In the gas phase, aminothiophenes and anilines are preferentially ring-protonated and nitrogen-protonated, respectively, but the energy gap is small and, as a consequence, the result depends largely on the theoretical method employed. In solution (whether in DMSO or water), N-protonation of anilines is clearly borne out, whereas the energy of the two protonated forms of aminothiophenes are essentially equal, although solvation strongly favors the ammonium ion. However, calculated NMR chemical shift changes only agree with N-protonation, which may then be regarded as the major process in solution for both base types. Hence, in this respect IPCM calculations are only partly successful, whereas calculated  $^{13}\text{C}$  nuclear shieldings allow a clear distinction of the two acid–base processes. The higher nucleophilic reactivity at C-2 of aminothiophenes does not stem from a lower aromaticity of the thiophene ring, but rather from a strong polarization of the C-2 $^{\delta-}$ –C-3 $^{\delta+}$  bond, which is present to a smaller extent in anilines because the electron density is shared between C-2 and C-4.

**Supporting Information Available:** Structures of **1–4** and associated protonated forms, calculated at the MP2(full)/6-31G-(d) level as PDB files. This material is available free of charge via the Internet at <http://pubs.acs.org>.

### References and Notes

- (1) (a) Pollack, S. K.; Devlin, J. L.; Summerhays, K. D.; Taft, R. W.; Hehre, W. J. *J. Am. Chem. Soc.* **1977**, *99*, 4583. (b) Summerhays, K. D.; Pollack, S. K.; Taft, R. W.; Hehre, W. J. *J. Am. Chem. Soc.* **1977**, *99*, 4585.
- (2) Lau, Y. K.; Nishizawa, K.; Tse, A.; Brown, R. S.; Kebarle, P. J. *Am. Chem. Soc.* **1981**, *103*, 6291.
- (3) Smith, R. L.; Chyall, L. J.; Beasley, B. J.; Kenttämaa, H. I. *J. Am. Chem. Soc.* **1995**, *117*, 7971.
- (4) Hillebrand, C.; Klessinger, M.; Eckert-Maksic, M.; Maksic, Z. B. *J. Phys. Chem.* **1996**, *100*, 9698.
- (5) Roy, R. K.; de Proft, F.; Geerlings, P. *J. Phys. Chem. A* **1998**, *102*, 7035.
- (6) Russo, N.; Toscano, M.; Grand, A.; Mineva, T. *J. Phys. Chem. A* **2000**, *104*, 4017.
- (7) Lee, S.-W.; Cox, H.; Goddard, W. A., III.; Beauchamp, J. L. *J. Am. Chem. Soc.* **2000**, *122*, 9201.
- (8) Bagno, A.; Bujnicki, B.; Bertrand, S.; Comuzzi, C.; Dorigo, F.; Janvier, P.; Scorrano, G. *Chem. Eur. J.* **1999**, *5*, 523.
- (9) (a) Outurquin, F.; Paulmier, C. *Bull. Soc. Chim. Fr. II* **1980**, 151. (b) Outurquin, F.; Paulmier, C. *Bull. Soc. Chim. Fr. II* **1983**, 153. (c) Outurquin, F.; Paulmier, C. *Bull. Soc. Chim. Fr. II* **1983**, 159. (d) Outurquin, F.; Lerouge, P.; Paulmier, C. *Bull. Soc. Chim. Fr.* **1986**, 259, 267. (e) Berkaoui, M.; Outurquin, F.; Paulmier, C. *J. Heterocycl. Chem.* **1996**, *33*, 9.
- (10) (a) Paulmier, C. *Sulfur Rep.* **1996**, *19*, 215. (b) Brugier, D.; Outurquin, F.; Paulmier, C. *Tetrahedron* **1997**, *53*, 103.
- (11) Verboom, W.; Berboom, C.; Eissink, I. M.; Lammerink, B. H. M.; Reinhoudt, D. N. *Recl. Trav. Chim. Pays-Bas* **1990**, *109*, 481.
- (12) Abdulla, R. F.; Fuhr, H. K. *J. Heterocycl. Chem.* **1976**, *13*, 427.
- (13) Terrier, F.; Pouet, M.-J.; Kizilian, E.; Hallé, J.-C.; Outurquin, F.; Paulmier, C. *J. Org. Chem.* **1993**, *58*, 4696.
- (14) Terrier, F.; Pouet, M.-J.; Gzouli, K.; Hallé, J.-C.; Outurquin, F.; Paulmier, C. *Can. J. Chem.* **1998**, *76*, 937.
- (15) (a) Buncel, E.; Renfrow, R. A.; Strauss, M. J. *J. Org. Chem.* **1987**, *52*, 488. (b) Strauss, M. J.; Renfrow, R. A.; Buncel, E. *J. Am. Chem. Soc.* **1983**, *105*, 2473. (c) Spear, R. J.; Norris, W. P.; Read, R. W. *Tetrahedron Lett.* **1983**, *24*, 1555. (d) Norris, W. P.; Spear, R. J.; Read, R. W. *Austr. J. Chem.* **1983**, *36*, 297. (e) Read, R. W.; Spear, R. J.; Norris, W. P. *Austr. J. Chem.* **1984**, *37*, 985.
- (16) Foresman, J. B.; Keith, T. A.; Wiberg, K. B.; Snoonian, J.; Frisch, M. J. *J. Phys. Chem.* **1996**, *100*, 16098.
- (17) Frisch, M. J.; Trucks, G. W.; Schlegel, H. B.; Scuseria, G. E.; Robb, M. A.; Cheeseman, J. R.; Zakrzewski, V. G.; Montgomery, J. A., Jr.; Stratmann, R. E.; Burant, J. C.; Dapprich, S.; Millam, J. M.; Daniels, A. D.; Kudin, K. N.; Strain, M. C.; Farkas, O.; Tomasi, J.; Barone, V.; Cossi, M.; Cammi, R.; Mennucci, B.; Pomelli, C.; Adamo, C.; Clifford, S.; Ochterski, J.; Petersson, G. A.; Ayala, P. Y.; Cui, Q.; Morokuma, K.; Malick, D. K.; Rabuck, A. D.; Raghavachari, K.; Foresman, J. B.; Cioslowski, J.; Ortiz, J. V.; Stefanov, B. B.; Liu, G.; Liashenko, A.; Piskorz, P.; Komaromi, I.; Gomperts, R.; Martin, R. L.; Fox, D. J.; Keith, T.; Al-Laham, M. A.; Peng, C. Y.; Nanayakkara, A.; Gonzalez, C.; Challacombe, M.; Gill, P. M. W.; Johnson, B.; Chen, W.; Wong, M. W.; Andres, J. L.; Gonzalez, C.; Head-Gordon, M.; Replogle, E. S.; Pople, J. A. *Gaussian 98*, Revision A.7; Gaussian, Inc.: Pittsburgh, PA, 1998.
- (18) Curtiss, L. A.; Ragavachari, K.; Redfern, P. C.; Rassolov, V.; Pople, J. A. *J. Chem. Phys.* **1998**, *109*, 7764.
- (19) Curtiss, L. A.; Redfern, P. C.; Ragavachari, K.; Rassolov, V.; Pople, J. A. *J. Chem. Phys.* **1999**, *110*, 4703.
- (20) Bagno, A.; Comuzzi, C. *Eur. J. Org. Chem.* **1999**, 287.
- (21) Bagno, A.; Modena, G. *Eur. J. Org. Chem.* **1999**, 2893.
- (22) Bagno, A.; Scorrano, G. *Acc. Chem. Res.* **2000**, *33*, 609, and references therein.
- (23) Bagno, A. *J. Phys. Org. Chem.* **2000**, *13*, 574.
- (24) Becke, A. D. *J. Chem. Phys.* **1993**, *98*, 5648.
- (25) Bagno, A.; Scorrano, G. *J. Phys. Chem.* **1996**, *100*, 1545.
- (26) Schleyer, P. v. R.; Maerker, C.; Dransfeld, A.; Jiao, H.; van Eikema-Hommes, N. J. R. *J. Am. Chem. Soc.* **1996**, *118*, 6317.
- (27) Reed, A. E.; Curtiss, L. A.; Weinhold, F. *Chem. Rev.* **1988**, *88*, 899.
- (28) Bagno, A.; Dorigo, F.; McCrae, P.; Scorrano, G. *J. Chem. Soc., Perkin Trans. 2* **1996**, 2163.
- (29) Hunter, E. P.; Lias, S. G. *J. Phys. Chem. Ref. Data* **1998**, *27*, 413 (<http://webbook.nist.gov>).
- (30) (a) Ewing, D. F. *Org. Magn. Reson.* **1979**, *12*, 499. (b) Bulbarela, A.; Tlahuext, H.; Morales, H. R.; Cuellar, L.; Uribe, G.; Contreras, R. *Magn. Reson. Chem.* **1986**, *24*, 1093.
- (31) (a) Gronowitz, S.; Hoffman, R. A. *Ark. Kemi* **1960**, *16*, 515. (b) Gronowitz, S.; Hoffman, R. A. *Ark. Kemi* **1960**, *16*, 539.
- (32) Takahashi, K.; Sone, T.; Fujieda, K. *J. Phys. Chem.* **1970**, *74*, 2765.